Implementing a bidirectional impulse turbine into a thermoacoustic refrigerator

Michael A. G. Timmer, Kees de Blok, and Theo H. van der Meer

Citation: The Journal of the Acoustical Society of America **148**, 1703 (2020); doi: 10.1121/10.0002001
View online: https://doi.org/10.1121/10.0002001
View Table of Contents: https://asa.scitation.org/toc/jas/148/3
Published by the Acoustical Society of America

JASA ARTICLE

Implementing a bidirectional impulse turbine into a thermoacoustic refrigerator

Michael A. G. Timmer,[1,a)] Kees de Blok,[2] and Theo H. van der Meer[1]
[1]*Department of Thermal Engineering, University of Twente, Enschede, The Netherlands*
[2]*SoundEnergy B.V., Enschede, The Netherlands*

ABSTRACT:
A thermoacoustic model is used to efficiently implement a bidirectional impulse turbine into a thermoacoustic refrigerator. Experiments are done for several gas types and mean pressures to identify its influence on the turbine efficiency. A scaling is investigated in an attempt to provide a unique function of the turbine efficiency for all operating conditions. Furthermore, the ratio of acoustic power absorbed by the turbine over to the total amount of available power is examined for varying conditions. Finally, the results are used to present a case study in which the turbine is used to drive the fluid pumps of the device. The remaining acoustic power is used for cooling, thus providing an off-grid thermoacoustic refrigerator that works purely with low-grade heat as an input.
 https://doi.org/10.1121/10.0002001

(Received 11 June 2020; revised 13 August 2020; accepted 7 September 2020; published online 23 September 2020)
[Editor: Philippe Blanc-Benon] Pages: 1703–1712

I. INTRODUCTION

Waste heat, or low-grade heat in general, can be converted into acoustic power using the thermoacoustic effect. Producing acoustic power in this manner can already be done for a heat source that is only 30 K higher than the environment.[1] The produced acoustic power is mostly used to provide refrigeration using the same thermoacoustic effect, thereby proving cooling using, e.g., solar heat[2] or waste heat,[3] without mechanically moving parts or harmful refrigerants. These thermoacoustic refrigerators only need electricity for pumps that circulate the working fluids through the internal heat exchangers. It is possible to use a part of the produced acoustic power, and convert it into electricity for these pumps, such that the thermoacoustic refrigerator works solely on the heat source.

So far, acoustic power has mostly been converted into electricity by using a kind of loudspeaker referred to as a linear alternator. This method is shown to be successful, but has its limits in scaling towards industrial sizes.[4] A promising alternative, especially for increasing scales, is the use of a bidirectional turbine to convert acoustic power into electricity. In oscillating water columns (OWCs), bidirectional turbines have been used to produce electric power up to the MW range.[5] In previous work, a bidirectional impulse turbine was characterized under thermoacoustic conditions to identify the relevant performance indicators, and provide rules of scaling.[6] Subsequently, the turbine has been optimized under thermoacoustic conditions to reach an efficiency of around 36%,[7] which is in the same order as found for OWCs.[8]

For both OWCs and the previous work, the turbine is used under atmospheric conditions with air as a working fluid. However, thermoacoustic devices generally work with helium or other noble gases at elevated pressures between 10 and 40 bar. Initial indications have shown that a bidirectional impulse turbine can reach an efficiency of 76% when used in a thermoacoustic device at a mean pressure of 10 bar.[9] In this work, this claim is investigated by implementing the same bidirectional turbine as used in the previous work[7] in a thermoacoustic refrigerator. The mean pressure and the type of gas will be varied to investigate the influence of it on the turbine efficiency. Furthermore, it is investigated whether the scaling derived for air at 1 bar[6] is still valid for different pressures and working fluids.

Details about the thermoacoustic refrigerator, bidirectional turbine, and the measurement procedure are given in Sec. II. A thermoacoustic model is presented in Sec. III, which is used to efficiently implement the turbine in the refrigerator in Sec. IV. This will mainly focus on the performance of the device as a whole, while implementing the electricity production besides the refrigeration. For the identified configuration, the performance of the bidirectional turbine is presented in Sec. V A for varying pressures and gases, while the performance of the complete device is treated in Sec. V B.

II. EXPERIMENTAL SET-UP

The bidirectional impulse turbine that will be used throughout this work is based on a design for an OWC.[10] Following the experiments from previous work under lab conditions,[7] the exact same turbine prototype will be implemented in a thermoacoustic device here. This turbine has a rotor shroud ring of 1 mm thickness, a tip clearance of

[a)]Electronic mail: timmer.mag@gmail.com, ORCID: 0000-0001-6008-8903.

0.3 mm, and an axial spacing between the guide vanes and the rotor of 1 mm. The shaft power produced by the turbine is converted into electricity by an electric motor (Hacker A10–13L, Hacker Motor GmbH, Ergolding, Germany) that is used as a generator. The three-phase power produced by the generator is dissipated in an electrical load consisting of sets of three precision resistors. To vary the turbine load for different operating conditions, four resistances can be used for the electrical load, namely R = 0.75, 2.0, 4.7, and 10 Ohm. The efficiency of the generator is calibrated for a varying turbine rpm with all electrical loads. The shaft power of the turbine, P_m, is calculated by dividing the measured electric power with the generator efficiency. More details on the turbine design, calibration, and measurement can be found in previous work.[6,7]

The turbine is implemented in a four-stage thermoacoustic refrigerator that is schematically shown to scale in Fig. 1. The two vessels that produce acoustic power are denoted as the engines, and the two vessels that provide cooling are depicted as the heat pumps. In each of the vessels, there are two heat exchangers that enclose the regenerator material in which the thermoacoustic effect occurs. In the engines, thermal oil is used as the heat source to produce the acoustic power. The input temperature, T_{in}, is measured and can reach up to 200 °C for the presented experiments. In the heat pumps, a water-glycol mixture is used as the medium to transfer the cold. Besides the hot and cold heat exchangers, each vessel has an ambient heat exchanger that uses water as a working fluid. To make a fair comparison between all experiments, the temperature of the cold circuit is kept near the ambient temperature, which is stable at 20 °C. The acoustic power is produced in the direction from the ambient heat exchanger to the hot heat exchanger, resulting in the acoustic power traveling through the device as depicted in Fig. 1. More details on how the acoustic power is exactly produced, as well as the design of the engines and heat pumps is beyond the scope of this work, but can be found in other literature on four-stage thermoacoustic engines.[1]

The turbine is implemented in the feedback tube between the second heat pump and the first engine, as shown in Fig. 1. In Sec. IV, this configuration is shown to provide the best performance in terms of produced acoustic power for the entire device. Note that for practical reasons, the turbine is implemented in a feedback tube with a 700 mm straight part (denoted as long), which is in contrast to the standard tubes with a 600 mm straight part (denoted as normal). To acoustically compensate for this extra length, a long feedback tube is also used between engine #1 and engine #2. All feedback tubes have a diameter of 54 mm, which is slightly less than the 60 mm diameter of the tube section in which the turbine is housed. The latter tube is used since this is a section of the experimental lab set-up from previous work,[6,7] which ensures that the turbine performance can be compared for an identical turbine and its mount. To connect the tubes with a different diameter, a rounded transition is made in the flange that connects the sections. In Sec. V A, it is shown that this transition causes some unwanted acoustic losses, which are accounted for in a single experiment to show the influence thereof.

To measure the input power to the turbine, the acoustic power is measured before and after it. This is done by using four piezoresistive pressure sensors (P1–P4) from First Sensor (First Sensor AG, Berlin, Germany) that have a range of 0 to 20 bar to deal with the varying pressure experiments. Using sets of two pressure sensors at the given distance, the local acoustic power is calculated using the method given by Fusco *et al.*[11] As shown in Fig. 1, a thermocouple is used to measure the temperature in the middle of the pressure sensors, such that the local gas properties for the acoustic power calculation can be accurately determined. Even though the turbine is placed at the ambient side of engine #1, the difference in temperature between both sides of the turbine can easily reach 5 °C. With the measurement of the acoustic power difference over the turbine, ΔE_2, and the shaft power produced by the turbine, the efficiency is calculated as $\eta_t = P_m/\Delta E_2$. Following previous work,[6] a function that uniquely determines the turbine efficiency is

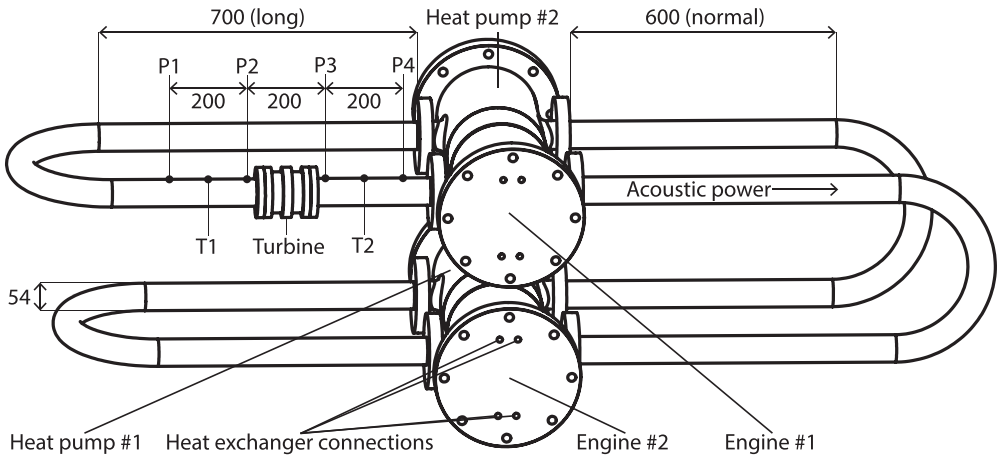

FIG. 1. Schematic of the thermoacoustic refrigerator with implemented bidirectional turbine (to scale). The pressure sensor locations (P1–P4) and tube dimensions are given in mm. A detailed design of the turbine can be found in previous work (Refs. 6 and 7).

https://doi.org/10.1121/10.0002001

found by scaling with the thermoacoustic input coefficient, C_{ta}, as follows:

$$C_{ta} = \frac{\Delta E_2^*}{\phi^3 + \phi^2}, \tag{1}$$

where ΔE_2^* is the acoustic power drop over the turbine scaled by $\rho N^3 D^5$, with ρ the density, N the rotation rate, and D the turbine diameter.[6] The flow coefficient ϕ is defined by the ratio of the axial gas velocity, c_x, over the blade speed, U, where the gas velocity is deduced from the pressure signals using the method given by Fusco *et al.*[11] More details about the calculation of these performance indicators can be found in previous work.[6]

During the experiments under varying operating conditions, it is found that the pressure amplitude ranges from about 2 to 20 kPa. Especially for the lowest amplitudes, this is quite small with respect to the resolution of the pressure sensors. This was found to be an issue for the phase difference between two adjacent pressure sensors, which initially varied significantly, resulting in an inaccurate calculation of the acoustic power. To deal with this issue, acoustic waveforms are sampled for 4 s instead of 1 s and sampled at 20 kHz, to more accurately determine the phase information. Furthermore, by increasing the input temperature of the hot oil relatively slowly, enough phase data are acquired to make an accurate fit of the phase difference between the pressure sensors as a function of the measured amplitude. This phase information is then used to calculate the acoustic power with sufficient accuracy. The latter is concluded from the fact that the results were found to be repeatable, and measuring with either increasing or decreasing oil temperature resulted in no significant difference when measuring slow enough. As an indication, each experiment presented in this work takes approximately one hour, in which the oil temperature is slowly raised from about 100 °C to 200 °C. The measurement points presented in this work are an average of twenty segments acquired by 4 s of sampling. The standard deviation of these averaged results is typically no more than 0.4% in turbine efficiency, which also decreases for increasing pressure amplitudes due to the relatively better resolution of the measurements. A typical measurement with this standard deviation as an error bar will be presented as the first result in Sec. V A.

III. THERMOACOUSTIC MODEL

In Sec. II, it is shown where the bidirectional turbine is eventually implemented in the thermoacoustic refrigerator. Since it is not straightforward to do this in thermoacoustic devices without harming its performance, this location has been determined by using a thermoacoustic model that can predict the performance of a system for a given design. In this section, details about the thermoacoustic model are presented. In Sec. IV, the model is validated with experiments, and subsequently used to determine the aforementioned location for the bidirectional turbine. In other work, a more elaborate description of the model[12] and its use for a practical application[13] can be found.

A successful model should be able to predict the pressure and flow rate in the entire device as a function of the temperature at the heat exchangers, where the latter can be regarded as control parameters. This can be done by splitting the entire system into smaller segments, for which a local representation is determined. This is often done by using an electrical analogy, where the pressure is regarded as a voltage and the flow rate as a current. For simple systems, each segment can then be described as a combination of electrical components, such as resistors, capacitors, and inductors. By combining all segments into an electrical network, it can be solved to find the pressure and velocity at all locations. However, the usefulness of such a method declines with the increased complexity of a system, especially when the segments are large with respect to the acoustic wavelength, such as for the feedback tubes.[12]

Similar to the electrical analogy, the model used in this work uses a lumped system of circuit elements, but here the individual segments are modeled with acoustic two-ports. The advantage of such a description for a segment is that only the transmission and reflection of the acoustic wave are of importance, while the inner workings can be regarded as a black box. This means that even if not all sections can be modeled analytically, the overall system can still be solved by experimentally measuring the transmission and reflection of the unknown segments individually, as is done for the entire system in this work. The latter is enough to fully characterize the elements, and this approach remains valid for segments that are large with respect to the acoustic wavelength.[12]

To describe the use of acoustic two-ports in more detail, two of them are depicted in Fig. 2 along with the local wave components. The acoustic two-ports are fully described by the four complex s-parameters, which are frequency dependent. For each acoustic wave reaching a two-port (from either side), the s-parameters determine how much of the wave is transmitted and reflected. For example, for the incident wave at the first two-port (i_1), the parameter s_{11a}

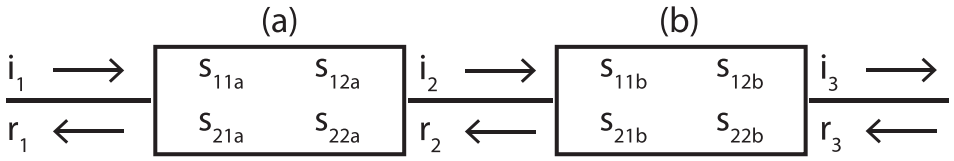

FIG. 2. A cascade of two acoustic two-ports in series, where the incident waves are denoted by i and the reflected waves by r. The s-parameters of the segments (a) and (b) fully determine the transmission and reflection of each two-port.

determines the reflected part, and s_{21a} the transmitted part. Similarly, for reflected wave (r_2) reaching this two-port from the right hand side, s_{22a} determines the reflected part and s_{12a} the transmitted part. By combining these effects, the local wave components around two-port (a) are described by a simple system of equations:

$$r_1 = s_{11a} i_1 + s_{12a} r_2, \tag{2}$$

$$i_2 = s_{21a} i_1 + s_{22a} r_2. \tag{3}$$

By rewriting these equations, they can be given in matrix-vector form as follows:

$$\begin{bmatrix} i_1 \\ r_1 \end{bmatrix} = \frac{1}{s_{21a}} \begin{bmatrix} 1 & -s_{22a} \\ s_{11a} & -\Delta s_a \end{bmatrix} \begin{bmatrix} i_2 \\ r_2 \end{bmatrix} = [\mathbf{S_a}] \begin{bmatrix} i_2 \\ r_2 \end{bmatrix}, \tag{4}$$

where $\Delta s_a = s_{11a} s_{22a} - s_{21a} s_{12a}$. This matrix-vector form is convenient because it allows one to simply cascade multiple two-ports. By applying the same method for two-port (b), the incident and reflected waves on both sides of the cascade are described by:

$$\begin{bmatrix} i_1 \\ r_1 \end{bmatrix} = [\mathbf{S_a}][\mathbf{S_b}] \begin{bmatrix} i_3 \\ r_3 \end{bmatrix} = [\mathbf{S_{ab}}] \begin{bmatrix} i_3 \\ r_3 \end{bmatrix}, \tag{5}$$

where $[\mathbf{S_{ab}}]$ follows from matrix multiplication, and determines the properties of an equivalent two-port for the entire cascade. Since this procedure can be repeated for an arbitrary amount of two-ports, the entire thermoacoustic device can be modeled by cascading all segments of the system. Note that from the components of the determined incident and reflected waves, the local pressure and flow rate can be found at all junction planes.[12]

To solve the system of two-ports that models the thermoacoustic device, only the s-parameters for all segments have to be known. For simple elements, they might be determined analytically, but since the s-parameters hold a physical meaning, they can also be measured.[12,14] For this work, only the segment with the bidirectional turbine has to be added to the existing model of the thermoacoustic refrigerator, which is based on experimental measurements. This has been done by implementing the turbine two-port as a function of the frequency and the acoustic power absorbed by the turbine, as measured in previous work.[7] With all the complex s-parameters known, and the given control parameters in the form of temperatures at all regenerators, the system can be solved. This is done by iteratively determining the correct operating frequency, pressure amplitude, and velocity amplitude for which the equivalent two-port of the entire system is in balance, where the latter equates to the reflection of the entire system (s_{11}) to be equal to one. This means that the acoustic signal at the input of the system is the same as at the output, and thus a steady-state operating point is found. The iterating procedure is started by identifying the operating frequency, which is found by sweeping over a range of frequencies and identifying the largest value of s_{11} for an initial pressure and velocity estimate. For the determined frequency, the velocity and, subsequently, the pressure amplitude are iterated to find a combination that yields $s_{11} = 1$, which is the steady-state operating point. In other words, the operating point is found for which the acoustic power that is added to the system at the engine stages, balances with the energy subtracted from the system by the heat pumps, the turbine, and the acoustic losses. Note that this is a solution to the thermoacoustic system, thus it relates the acoustic power to the internal temperatures. By using the measured performance of the gas-fluid heat exchanger as a function of the acoustic velocity and fluid flow rate through it, this is converted into the external temperatures of the fluid circuits. In this latter form, the model calculates the performance of the system in parameters that are practically relevant, and can be measured for the actual thermoacoustic device.

IV. TURBINE IMPLEMENTATION

This section will focus on validating the thermoacoustic model with experimental results and, subsequently, using the model to implement a bidirectional turbine in a thermoacoustic refrigerator. The success of implementation is quantified by looking at the performance of the complete device. For a given input temperature of the hot oil, a higher level of acoustic power running through the machine is regarded as a better implementation of the turbine. In Sec. V, the performance of the turbine itself will be presented for the best implementation that is identified in this section.

As a benchmark for the turbine implementation, the performance of the refrigerator without a turbine is calculated using the thermoacoustic model, and measured experimentally. The resulting acoustic loop power as a function of the input temperature of the oil is presented in Fig. 3. Just as for all other cases in this section, the given results are for air with a mean pressure of 10 bar. The first thing that can be seen for the case with no turbine is that the model matches the experimental results relatively well. The two things that should mainly be examined are the onset temperature at which the first acoustic power is produced, and the slope of the acoustic power curve for subsequently increasing temperature. Both of these characteristics also hold a physical meaning, where the onset temperature quantitatively indicates how well the device is acoustically matched, since a low onset temperature means that even a small acoustic signal can already be sustained in the given device. The slope is a measure for the acoustic losses in the system. The latter also includes the acoustic power that will be absorbed by the turbine, which is why the slope of the curves with a turbine will not be as steep as the one without a turbine. However, ideally the acoustic matching for a device with a turbine is such that the onset temperature of 70 °C for the case with no turbine is still reached.

For initial tests, the 700 mm feedback tube, including the bidirectional turbine, is implemented with the turbine near the second heat pump (see HP #2 in Fig. 1). All other feedback tubes have been kept at the normal length of

https://doi.org/10.1121/10.0002001

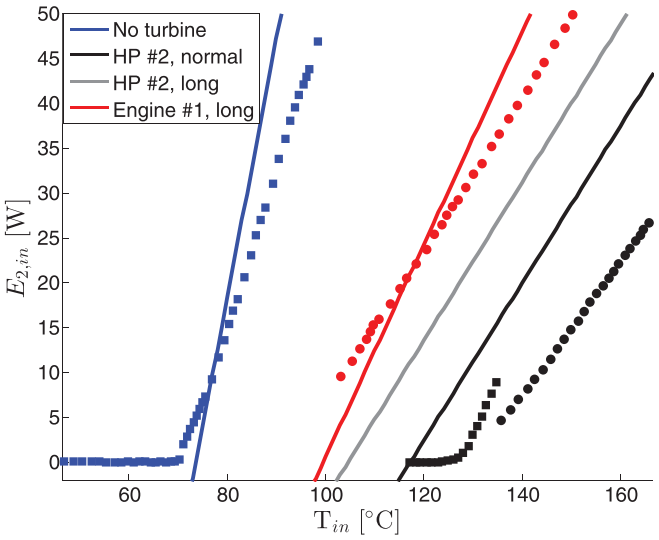

FIG. 3. (Color online) Acoustic power in front of the turbine section as a function of the oil input temperature. The solid lines represent results from the thermoacoustic model, while the markers denote experimental results. The bullets (●) represent a working turbine and the square markers (■) are for the turbine either not running yet or not being present at all. The legend denotes the turbine location, which is just after the second heat pump (HP #2) or in front of engine #1, as depicted in Fig. 1. It further describes the length of the feedback tube between engine #1 (with turbine) and engine #2 (without turbine), which is either the normal 600 mm or the longer 700 mm length.

600 mm. Using this configuration, it is found that the bidirectional turbine can indeed produce electric power inside the thermoacoustic refrigerator, yet only at a low level. It can be seen in Fig. 3 that both the model and experiments show that the onset temperature of the device is significantly increased due to the implementation of the turbine. The experimentally measured 125 °C onset temperature is indicative of bad acoustic matching, and should be improved by implementing the turbine differently. What is interesting to see from the experimental results though, is that the slope of acoustic power increase is similar to the case of no turbine at the moment when the turbine is not yet running. Once there is sufficient power such that the turbine self-starts, the acoustic loop power drops, and the slope decreases since the turbine is absorbing acoustic power (and converting it into electricity). The slope is now approximately equal to the predicted value by the model, which does not account for the starting behavior of the turbine.

With some good indications that the thermoacoustic model can be used to predict trends in the performance of the device, it is used to search for a better implementation of the turbine. An evident attempt to improve the acoustic matching is to account for the extra tube length introduced by the turbine. It can be seen in Fig. 3 that the predicted onset temperature is significantly lower when a longer feedback tube is introduced between engines #1 and #2. Besides this, the location of the turbine and the extra feedback tube have been varied in the model to find the optimal configuration. The latter was found by keeping the additional longer tube in place, while moving the turbine to the position just before engine #1, as depicted in Fig. 1. It is experimentally shown that this implementation is indeed significantly better than the initial attempt, since the onset temperature can now be extrapolated to be approximately 85 °C. Note that this is not yet on par with the case of no turbine, which is most likely caused by the presence of the turbine in only one of the long tubes, still resulting in some acoustic mismatch. This might be solved by using a dummy load in the feedback tube between engines #1 and #2, but this will also introduce additional acoustic losses that lower the slope. Therefore, the configuration of the device is kept as shown in Fig. 1 in the remainder of this work, which will ensure enough acoustic power for the turbine to be investigated for a large range of operating conditions.

The results presented in this section indicate that the thermoacoustic model is a useful tool in predicting the performance of a device in question. Even though the absolute value of the acoustic power can still vary significantly, it is shown that the predicted trends are in accordance with experimental results. The latter makes the model sufficiently useful, since the main purpose of the model is only to guide in designing and optimizing thermoacoustic devices. Another useful property of the model is to predict the operating frequency of the machine. For the given turbine implementation, the frequency with air as a working fluid is calculated to be 23.4 Hz, which is confirmed by the experiments. Predicting the operating frequency is especially useful to determine the ratio of gas mixtures, without having to accurately measure how much gas is added. Since the speed of sound is different for air, helium, and argon, which will be used in this work, it is possible to determine the mixture ratio of two gases from the experimentally measured frequency. The gas mixtures that are used in Sec. V are determined in this manner. Finally, it is worth noting that both the model and experimental results for different gas types provide the same conclusions about the turbine implementation as presented for air in this section.

V. RESULTS

In this section, the performance of the implemented turbine is investigated for a wide range of operating conditions. The pressure of the working fluid will be varied from 10 bar down to 3 bar, which is the limit at which there is still sufficient acoustic power available for the turbine. Sweeps of increasing oil temperature are performed for several generator loads at each pressure. Furthermore, helium, argon, and an air-helium mixture are used as a working fluid besides air. As described in Sec. IV, the ratio of the air-helium mixture is determined from the measured frequency of 36.5 Hz, yielding a mass ratio of 40% air and 60% helium. Note that for the full helium and argon measurements, there is still air at ambient pressure left in the device when filling, which accounts for approximately 10% of the mass. This is accounted for in calculating the acoustic power, but for clarity the mixtures are simply referred to as pure helium and argon. For the varying operating conditions, Sec. V A will

start with examining the turbine efficiency as a function of the acoustic power absorbed by the turbine. Subsequently, it is investigated whether scaling the performance using Eq. 1 still holds for varying gas types and pressures. In Sec. V B, the refrigerator and turbine combination are considered as a whole, looking at the amount of acoustic power absorbed by the turbine and thus, how much is left over for refrigeration purposes.

A. Turbine performance

Figure 4 presents the turbine efficiency for a measurement with helium at the given pressure and generator load, along with the standard deviation of the averaged results as an error bar. It can be seen that the maximum turbine efficiency is approximately 32%, which is significantly less than the 36% that was measured under lab conditions in previous work for air at 1 bar.[7] This difference could be caused by the different operating conditions, but later in this section it is shown that this is not the case. The fact that the measured efficiency is lower is actually caused by the transition from a 54 mm tube to a 60 mm tube in the flanges around the turbine section (see Fig. 1), which was not present in the set-up of the previous work. This transition introduces some additional acoustic losses, which are incorrectly ascribed to the absorbed acoustic power of the turbine since the measurement is done in the 54 mm tubes. To identify the magnitude of these losses, the experiment is repeated without a turbine using the same set-up. The loss in acoustic power between the upstream and downstream measurement is found to linearly increase as a function of the acoustic loop power, and reach approximately 2 W at a loop power of 100 W. By subtracting the acoustic losses as a function of the current loop power, the turbine efficiency is recalculated and shown in Fig. 4 as well. With this correction, the maximum turbine efficiency is now just above 36%, which is in the same range as the previous measurements. Nevertheless, the results in the remainder of this work are presented without such a correction, since it is not deemed necessary for comparing the turbine efficiency as a function of varying operating conditions.

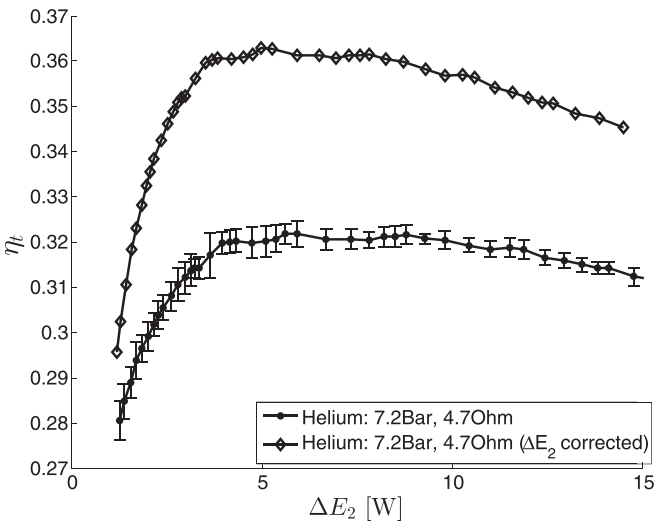

FIG. 4. Turbine efficiency as a function of the acoustic power absorbed by the turbine. The legend depicts the operating conditions, where the corrected results represent turbine efficiency as calculated when incorporating a correction for the acoustic losses at the tube transitions. The error bars for the normal results depict the standard deviation of averaging 20 measurement points for each given turbine efficiency.

Following the previous measurement with helium, it is interesting to see how increasing and decreasing the mean pressure in the device will influence the turbine efficiency. In Fig. 5, the turbine efficiency is given for measurements with three different mean pressures using helium. It can be seen that the maximum turbine efficiency remains constant at 32% when decreasing the mean pressure from 7.2 to 4.8 bar. The maximum turbine efficiency also does not vary when further increasing the mean pressure and changing the load to the generator. From this it can be concluded that the mean pressure in the device does not affect the maximum turbine efficiency. This is in contrast with the rising efficiency for increasing mean pressure shown in other work,[9] where a 76% turbine efficiency is reached at 10 bar. Correspondence about the measurement procedure from this other work has provided additional details that are not available in literature. This revealed that the acoustic power in front of the turbine was not directly measured, but estimated from the pressure amplitudes in the vessels using a model similar to the one presented in Sec. III. Furthermore, assumptions are made about the amount of acoustic power that is absorbed by the turbine, while this is heavily dependent on the operating conditions, as will be shown in Sec. V B. Due to these estimations, it is likely that the measurements in the current work provide more realistic results, since the acoustic power is directly measured on both sides of the turbine. Therefore, it can be said that the maximum turbine efficiency is actually not dependent on the mean pressure of the working fluid.

Since it is determined that there is no influence of the generator load and the mean pressure, it is allowed to vary these in an attempt to reach a maximum in turbine

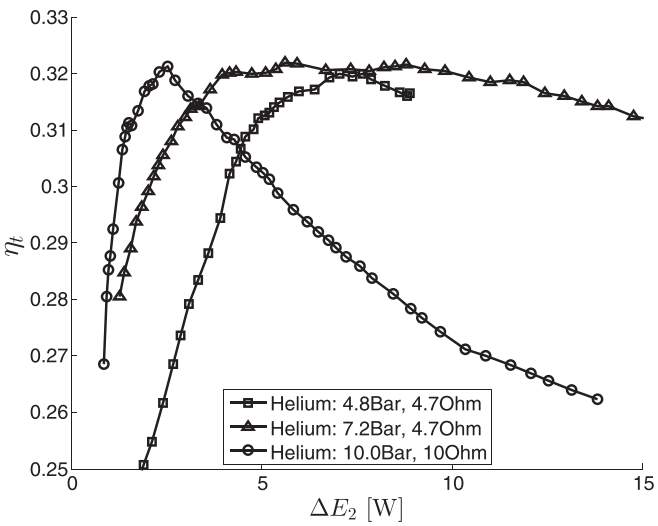

FIG. 5. Turbine efficiency as a function of the acoustic power absorbed by the turbine. The legend depicts the operating conditions for the different measurements with helium.

https://doi.org/10.1121/10.0002001

efficiency, while still making a fair comparison between different working fluids. The results for such a study are given in Fig. 6, where the turbine efficiency is given for measurements with helium, air, argon, and the air-helium mixture for varying generator loads and mean pressures. It can be seen that, despite the wide range in operating conditions, the maximum turbine efficiency is still around 32% for all cases. Therefore, it can be concluded that the type of working fluid also has no influence on the maximum turbine efficiency. Note that the acoustic frequency varies from 22 Hz for argon to 53 Hz for helium, thus showing that the frequency also has no influence on the maximum turbine efficiency, confirming what was measured in previous work for a single gas type and pressure.[6]

Besides the maximum turbine efficiency, the previous work showed that over the entire measurement range, the turbine efficiency can be scaled uniquely with the thermoacoustic input coefficient,[6] as given in Eq. 1. Since the present work also varies the gas type and the mean pressure, next to the acoustic frequency and generator load, it is interesting to see whether this scaling still holds. Figure 7 presents the turbine efficiency as a function of the thermoacoustic input coefficient for all results that have been presented so far, thus including the measurement for which the acoustic power is corrected. This latter result is interesting since it can be compared with the measurement from previous work under lab conditions,[6] which is also shown in Fig. 7. Focusing first on the results from this work, it can be seen that scaling with the thermoacoustic input coefficient works relatively well. Considering that for all operating conditions there is a wide spread in turbine efficiency as a function of ΔE_2, using C_{ta} as a performance indicator provides an almost unique function of the turbine efficiency. However, it is hard to conclude whether this scaling exactly holds, since a discrepancy of a few percent in C_{ta} is clearly visible between the different results. By checking additional

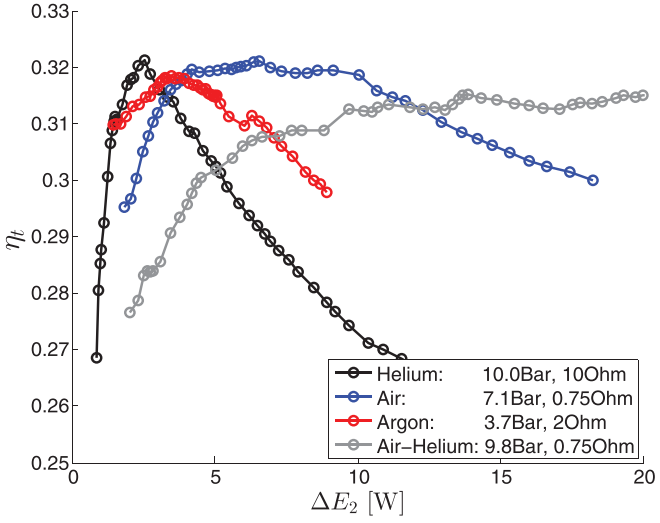

FIG. 6. (Color online) Turbine efficiency as a function of the acoustic power absorbed by the turbine. The legend depicts the operating conditions for the different measurements with helium, air, argon, and an air-helium mixture.

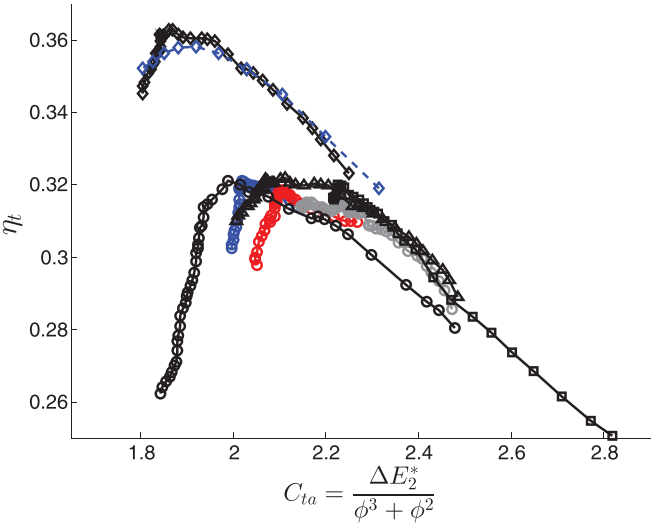

FIG. 7. (Color online) Turbine efficiency as a function of the thermoacoustic input coefficient. Details about the operating conditions of the different measurements can be found in the legends of Figs. 4, 5, and 6. The dashed line with diamond markers represents the measurement with air at 1 bar and 10 Ohm generator load from previous work (Ref. 7).

measurements that are not shown in this work, no consistent trend in either gas type or pressure was found. This leaves the acoustic power losses in the tube transition as a possible explanation for the slight differences in scaling. Comparing the measurement with corrected acoustic power to the lab results, quite a good agreement is found in turbine efficiency, especially since the gas type, mean pressure, generator load, and acoustic frequency are all different for these measurements. This shows that the thermoacoustic input coefficient can likely still be used to find the maximum turbine efficiency for any operating conditions. More confidence in such a conclusion could be provided by similar measurements that do not need any correction for the acoustic power.

B. Combined performance

The results presented so far have purely focused on the turbine, without regarding the entire device under varying operating conditions. For the latter, not only the efficiency of the turbine is of importance, but also the amount of acoustic power that is absorbed with respect to the total amount available. This is especially true for a combination such as the present device, since any acoustic power that is absorbed by the turbine is not available for refrigeration purposes anymore. In the following, the acoustic power absorption is given for a varying load, mean pressure, and gas type, after which the power distribution in the entire device is examined under typical thermoacoustic conditions.

In Fig. 8(a), the ratio of the absorbed acoustic power over the total amount of loop power is given for a varying load to the generator. First of all, it can be seen that for a given load, relatively more acoustic power is absorbed as the loop power increases. Second, for an available amount of acoustic loop power, the turbine absorbs more as the

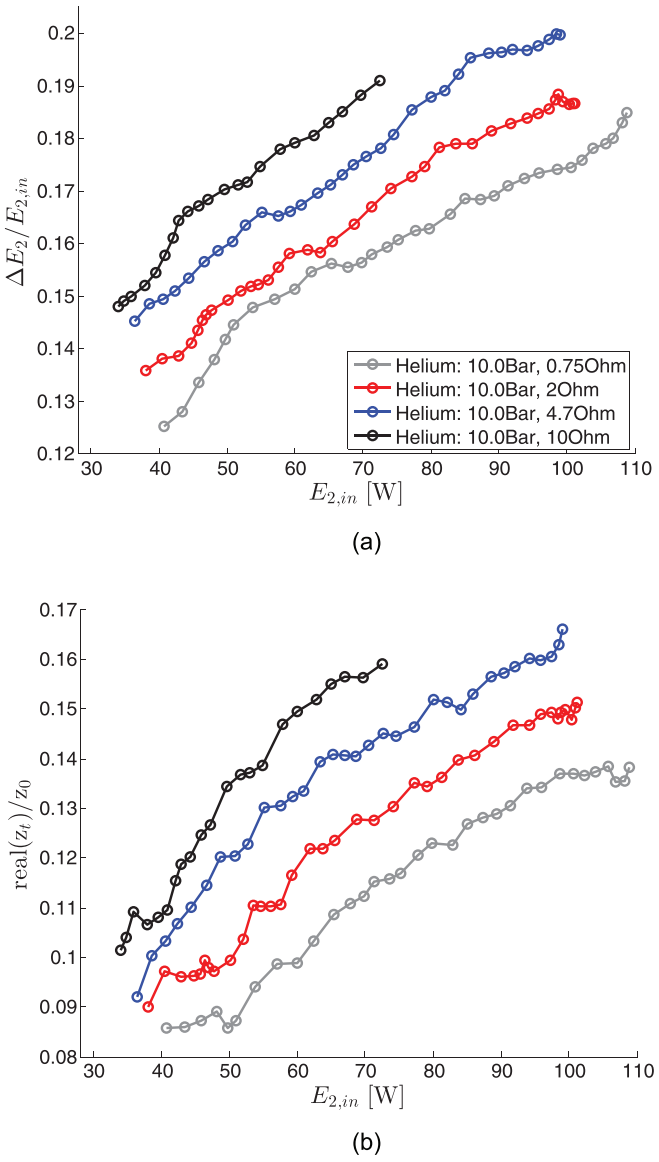

FIG. 8. (Color online) The ratio of absorbed acoustic power over input power (a) and the real part of the normalized turbine impedance (b) as a function of the acoustic loop power in front of the turbine. Results are presented from the point where the turbine absorbs at least 5 W acoustic power. The legend depicts the generator load for the measurements with helium at 10.0 bar mean pressure.

resistance to the generator is increased. Note that increasing the resistance means that the load to the turbine is actually reduced, thus increasing the rpm for given operating conditions. To explain the aforementioned two effects in acoustic power absorption, the real part of the normalized turbine impedance is presented in Fig. 8(b) for the same measurements. The real part of the turbine impedance can be regarded as the flow resistance, and it can be seen that it has a clear correlation with the amount of acoustic power that is absorbed. In previous work,[6] it was shown that increasing the turbine rpm causes a larger real part of the turbine impedance and, therefore, more acoustic power absorption. Since the rpm will increase for both a larger acoustic loop power and an increased load resistance for a given loop power, the larger associated impedance explains why more acoustic power is absorbed by the turbine for such conditions.

This section started by presenting results for a varying generator load, since this is the main way to vary the absorbed acoustic power during operation. This is typically necessary when the thermoacoustic device does not operate at a single point, e.g., due to fluctuations in the (low-grade) heat source or the ambient temperature. However, as can be seen in Fig. 8(a), the difference in absorbed acoustic power by the turbine is only a few percent between the largest and smallest load. Furthermore, to ensure a high efficiency, the flow conditions should be such that the turbine operates around the right thermoacoustic input coefficient (see Fig. 7). Due to this limited range of tuning possibilities during operation, it should be made sure that the acoustic power absorption is already around the required value. When large changes are needed for the latter, the turbine can be placed in an entirely different impedance region of the device, such as a perpendicular tube section, often referred to as a stub. Furthermore, the gas type and the mean pressure can also have a large influence on the absorbed acoustic power, as will be shown for a single turbine position next.

Table I presents the absorbed acoustic power ratio and real part of the normalized turbine impedance for varying generator load, mean pressure, and gas type. The results are given at an acoustic loop power of 50 W, which is chosen since it is the largest power that could be reached for 3.4 bar air. The values for the varying generator load at 10 bar helium correspond to the measurements presented in Fig. 8. Just as the results with a varying load, it can be seen from Table I that changes in the absorbed acoustic power for the other measurements again correlate with the real part of the turbine impedance. When reducing the mean pressure of air from 9.6 to 3.4 bar, the ratio of absorbed acoustic power increases from 0.19 up to 0.28. This shows that the mean pressure of the device has a big influence on the relative amount of acoustic power that is absorbed, while in Fig. 5 it is shown that there is no influence on the maximum turbine efficiency. Note that although thermoacoustic devices will generally not operate at these smallest pressures, they do often run at a mean pressure significantly larger than 10 bar, which would result in a smaller amount of absorbed acoustic power. The remaining results that are given in Table I are for varying gas types with 2 Ohm generator load and a mean pressure of approximately 10 bar. The results show that the ratio of absorbed acoustic power increases from 0.15 for helium up to 0.21 for argon, between which are the values for the air-helium mixture and pure air. Since helium has the smallest characteristic impedance (z_0), followed by air and finally argon, this indicates that relatively more acoustic power is absorbed as the characteristic impedance of the working fluid increases.

Now that the acoustic power absorption and the performance of the turbine have been identified for a wide range of operating conditions, there is enough information to apply this to practical use cases. As an example, a case study is

https://doi.org/10.1121/10.0002001

TABLE I. The real part of the normalized turbine impedance, real(z_t)/z_0, and the ratio of absorbed acoustic power over input power, $\Delta E_2/E_{2,in}$, for varying operating conditions. Results are given at 50 W acoustic loop power for a varying gas type, mean pressure, P_m, and generator load, R.

Gas	Pm (bar)	R (Ohm)	real(zt)/z0	$\Delta E_2/E_{2,in}$
Helium	10.0	0.75	0.09	0.14
	10.0	2	0.10	0.15
	10.0	4.7	0.12	0.16
	10.0	10	0.14	0.17
Air	9.6	2	0.18	0.19
	7.1	2	0.21	0.21
	5.4	2	0.24	0.24
	3.4	2	0.26	0.28
Air-Helium	9.8	2	0.14	0.18
Argon	9.8	2	0.19	0.21

TABLE II. Performance of the thermoacoustic refrigerator as a function of the input temperature of the heat source. The acoustic loop power, $E_{2,in}$, is derived from the measurements for the air-helium mixture at 9.8 bar with a 2 Ohm load. With 62 W of loop power absorbed by the turbine, 20 W of electricity is produced to run the pumps. The remaining acoustic power is converted into cooling power, Q_{cold}. With the input power from the heat source, Q_{in}, the COP is defined as Q_{cold}/Q_{in}.

T_{in} (°C)	Q_{in} (W)]	$E_{2,in}$ (W)]	Q_{cold} (W)]	COP
163	249	62	0	0
175	285	83	34	0.12
200	360	120	93	0.26
225	435	158	154	0.35
250	510	195	213	0.42
200	360	120	192[a]	0.53[a]

[a]Value when no turbine is present, and the pumps are driven by external power.

presented for the thermoacoustic refrigerator with electricity production that is treated in this work. The amount of electricity produced by the turbine will be set such that it can exactly power the three pumps that are needed for the fluid circuits of the heat exchangers. This provides an off-grid system, for which, in this case, all of the remaining acoustic power will be used to provide refrigeration in the heat pumps. Note that, similar to the current study, one can also use the remaining acoustic power to (partly) produce additional electricity.

The case study is based on the measured values for the air-helium mixture at 9.8 bar mean pressure with a 2 Ohm generator load. To provide an energy balance of the system, the input power of the heat source, Q_{in}, and the cooling power, Q_{cold}, have to be known. Since these are not measured during the turbine experiments, the input temperature and acoustic loop power are used to estimate these from measurements for a similar, yet significantly larger, four-stage thermoacoustic refrigerator. For the cooling power, this is done by using the acoustic power that is left after the turbine has used enough to produce electricity for the pumps. Since the latter is around 20 W, there is 62 W of acoustic power needed for the turbine when assuming a generator efficiency of 90% and a turbine efficiency of 36%. From the measurement with the air-helium mixture, it is found that 31 W of acoustic power is absorbed by a single turbine when the input temperature is around 200 °C. Therefore, using two turbines will provide exactly enough electricity for the pumps at this operating point, while using two turbines will also have the added benefit of a better acoustic matching (as described in Sec. IV). For the other input temperatures that are considered in the case study, it is assumed that one or several turbines can be used such that they absorb 62 W of acoustic power as well.

Table II presents the results of the case study, where the performance of the off-grid thermoacoustic refrigerator is given as a function of the input temperature of the heat source. The first thing to notice is that an input temperature of at least 163 °C is needed to run the system. For this input temperature and corresponding input power, just enough acoustic power is produced such that the turbines can power the pumps. Since the pump power does not change, increasing the input temperature from this point onwards will provide a surplus of acoustic power that can be used for refrigeration. A way to quantify the refrigeration performance is to look at the ratio of cooling power over the input power, which is defined as the coefficient of performance (COP). For 175 °C input temperature the COP is only 0.12, but it can be seen that this quickly rises with increasing temperature. As a comparison, it is shown in Table II that for a 200 °C input temperature, a COP of 0.53 is acquired when all acoustic power is used for refrigeration (in which case external power is of course needed for the pumps). In the off-grid version, approximately half of this performance is still reached at 200 °C. Furthermore, as the input temperature is further increased, the pump power becomes less relevant, and the COP of the off-grid version will converge towards the refrigeration only version. What will remain is the added capital costs of the machine due to the additional components producing electricity. Depending on the specific use case, it should be determined whether the added cost and complexity of the off-grid system is worth it. This might especially be the case for remote locations where the electricity grid is not stable or even present. For such cases, where the possibility of running off-grid is critical, a refrigerator working purely on a heat source could be much preferred over conventional systems.

VI. CONCLUSIONS

To implement a bidirectional impulse turbine into a thermoacoustic refrigerator, a model is presented that can predict the acoustic power in the device as a function of the input temperature. The thermoacoustic model is experimentally validated for configurations both with and without a turbine. Subsequently, the model is used to implement the turbine at a good location in the device, hereby focusing on the acoustic matching quantified by the onset temperature where oscillations start. For the identified turbine implementation, sufficient acoustic power can be generated by the

device to investigate the turbine under a wide range of operating conditions. In future work, more effort should be taken to implement the turbine with a better acoustic matching, which can, e.g., be done by adjusting more feedback tube sizes, or introducing a second turbine to form a matching pair.

For the implemented turbine with helium as a working fluid, it is shown that electric power can indeed be produced in the thermoacoustic refrigerator. After correcting for acoustic losses at two flange connections, the maximum efficiency of the turbine is found to be 36%, which is equal to the measured efficiency for the same turbine in previous lab experiments.

The mean pressure in the device is varied, which resulted in no significant change in the maximum turbine efficiency. This is found to be in contrast with other work, where the efficiency drastically increases as a function of the mean pressure. It is concluded that the results from this work are most likely correct, since the acoustic power to the turbine was more correctly measured in a direct manner. Besides the mean pressure, the generator load and the gas type were also varied. For helium, air, argon, and an air-helium mixture, the maximum turbine efficiency was found to be approximately the same for all pressures and generator loads. This constant maximum efficiency is convenient when designing a thermoacoustic engine, since the gas type and mean pressure can be chosen such that they are optimal for the rest of the device. Furthermore, this shows that the bidirectional turbine can be further optimized under lab conditions, after which the same performance can be expected with actual thermoacoustic conditions.

For all measurements under varying operating conditions, it is shown that the turbine efficiency is approximately a unique function of the thermoacoustic input coefficient. Furthermore, for the measurement with corrected acoustic power, a good agreement is found with the results from previous work under drastically different conditions. This indicates that this scaling can be used to identify the point at which the turbine operates at its maximum efficiency. Besides the most efficient point, it is shown how much acoustic power the turbine absorbs for the varying operating conditions. The acoustic power absorption is shown to be directly correlated with the real part of the normalized turbine impedance. By taking both the measures for the maximum turbine efficiency and the absorbed acoustic power into account, the turbine can be correctly implemented in a thermoacoustic device.

A case study is given which shows such an implementation, where the turbine is used to produce enough electric power to drive the fluid pumps, while the remaining acoustic power is used for refrigeration. The threshold for operation of the given device is found to be 163 °C for the temperature of the heat source. As the input temperature is increased above this value, the amount of cooling power and the COP rise, while the acoustic power needed for the turbine to drive the pumps becomes increasingly less relevant. The given case study shows that a thermoacoustic refrigerator running purely on a heat source is a viable option, especially when there is a need for off-grid operation.

[1]K. de Blok, "Novel 4-stage traveling wave thermoacoustic power generator," in *ASME 2010 3rd Joint US-European Fluids Engineering Summer Meeting collocated with 8th International Conference on Nanochannels, Microchannels, and Minichannels*, Montreal, Quebec, Canada (August 1–5, 2010), pp. 73–79.
[2]R. Chen and S. L. Garrett, "A large solar/heat-driven thermoacoustic cooler," J. Acoust. Soc. Am. **108**(5), 2554–2554 (2000).
[3]D. L. Gardner and C. Q. Howard, "Waste-heat-driven thermoacoustic engine and refrigerator," in *Proceedings of Acoustics 2009*, Adelaide, Australia (November 23–25, 2009), pp. 1–4.
[4]M. A. G. Timmer, K. De Blok, and T. H. Van Der Meer, "Review on the conversion of thermoacoustic power into electricity," J. Acoust. Soc. Am. **143**(2), 841–857 (2018).
[5]A. F. Falcão and J. C. Henriques, "Oscillating-water-column wave energy converters and air turbines: A review," Renew. Energy **85**, 1391–1424 (2016).
[6]M. A. G. Timmer and T. H. van der Meer, "Characterization of bidirectional impulse turbines for thermoacoustic engines," J. Acoust. Soc. Am. **146**(5), 3524–3535 (2019).
[7]M. A. G. Timmer and T. H. van der Meer, "Optimizing bidirectional impulse turbines for thermoacoustic engines," J. Acoust. Soc. Am. **147**(4), 2348–2356 (2020).
[8]T. Setoguchi, S. Santhakumar, H. Maeda, M. Takao, and K. Kaneko, "A review of impulse turbines for wave energy conversion," Renew. Energy **23**(2), 261–292 (2001).
[9]K. de Blok, P. Owczarek, and M. X. François, "Bi-directional turbines for converting acoustic wave power into electricity," in *9th PAMIR International Conference on Fundamental and Applied MHD*, Riga, Latvia (2014), pp. 433–438.
[10]M. Suzuki, M. Takao, E. Satoh, S. Nagata, K. Toyota, and T. Setoguchi, "Performance prediction of OWC type small size wave power device with impulse turbine," J. Fluid Sci. Technol. **3**(3), 466–475 (2008).
[11]A. M. Fusco, W. C. Ward, and G. W. Swift, "Two-sensor power measurements in lossy ducts," J. Acoust. Soc. Am. **91**(4), 2229–2235 (1992).
[12]K. de Blok and R. F. M. van den Brink, "Full characterization of linear acoustic networks based on N-ports and S Parameters," J. Audio Eng. Soc **40**(6), 517–523 (1992).
[13]K. de Blok, "Low operating temperature integral thermo acoustic devices for solar cooling and waste heat recovery," in *Proceedings of Acoustics 2008* Paris, France (June 29–July 4, 2008), pp. 3545–3550.
[14]K. de Blok and R. F. M. van den Brink, "Direct-reading one-port acoustic network analyzer," J. Audio Eng. Soc **41**(4), 231–238 (1993).